Optical, electrical and structural properties of sol gel ZnO:Al coatings

T. Schuler, M.A. Aegerter*

Department of Coating Technology, Institut für Neue Materialien (INM), Im Stadtwald Geb.43, D-66123 Saarbrücken, Germany

Abstract

Single and multilayer transparent conducting aluminium doped zinc oxide films have been prepared on DESAG AF45 substrates by the sol gel dip coating process. Zinc acetate solutions of 0.1–0.5 M in isopropanol stabilised by diethanolamine and doped with a concentrated solution of aluminium nitrate in ethanol were used. Each layer was fired at 600°C in a conventional furnace for 15 min. The final coatings were then tempered under a flux of forming gas (N_2/H_2) at 400°C for 2 h. The coatings have been characterised by surface stylus profiling, optical spectroscopy (UV-NIR), X-ray diffraction (XRD), transmission electron microscopy (TEM) and combined Hall and van der Pauw techniques. Single layers with thickness, d, ranging from 25 to 186 nm are polycrystalline with the zincite structure and exhibit a small preferential orientation with the (002) direction perpendicular to the surface (texture coefficient, TC, ranging from 1.8 to 2.8). They consist of almost spherical particles with size ranging from 15 to 25 nm (thin sample) to 40 nm (thick sample) with crystallite sizes ranging from 23 to 40 nm (002), respectively. The film resistivity decreases from 5×10^{-1} Ω cm ($d = 25$ nm) to 4×10^{-2} Ω cm ($d = 186$ nm). Multilayer coatings built with about 20 nm thick layers are also slightly textured along the (002) direction (TC ranging from 1.9 to 2.8). A structural evolution in morphology from spherical to columnar growth was observed. The crystallite size calculated from the (002) reflex increases with the number of layers from 23 nm for a single layer to over 100 nm for ten layers. The resistivity decreases from 5×10^{-1} Ω cm for a single layer to 5×10^{-3} Ω cm for ten layers ($d = 174$ nm). A model for the growth of the crystallites in sol gel multilayer coatings is presented.

Keywords: Zinc oxide; Sol gel; Multilayers; Structural properties; Electrical properties

1. Introduction

Aluminium doped zinc oxide (AZO) coatings exhibit high transparency and low resistivity and this material is suitable for the fabrication of solar cells [1] and flat panel display electrodes [2]. They also find applications as surface acoustic devices [3], optical waveguides [4], gas sensors [5] and micro-machined actuators [6].

Doped and undoped ZnO thin films have been prepared by physical deposition methods such as laser deposition [7], different sputtering methods [1,3,8,9], atomic layer deposition [2] and chemical deposition methods such as chemical vapour deposition [6], spray pyrolysis [10], chemical bath deposition [11] and the sol gel process [12–19]. A recent compilation of the properties of sol-gel derived AZO films is given in [15]. The reported resistivities vary from 7×10^{-4} [16] to 10 Ω cm whereas the reported resistivities of sputtered films are as low as 1×10^{-4} Ω cm [20]. These large discrepancies are currently not well understood.

The aim of this work is to investigate the influence of the multilayer deposition process on the structural, electrical and optical properties of sol gel ZnO:Al coatings as it is established that the fabrication process governs the microstructure [21] and influences the intrinsic properties of this material.

2. Preparation

The preparation of the coating solutions is shown in Fig. 1. Diethanolamine (DEA, Fluka puriss.) was first dissolved in isopropanol (iPrOH). Then zinc acetate dihydrate (ZnAc, Fluka puriss) was added under stirring. Doping of the solution was obtained by adding a 0.2 M solution of aluminium nitrate nonahydrate (Fluka puriss.) in ethanol in order to obtain a ratio Al/Zn = 0.6 at.%. Finally iPrOH was added to achieve the desired concentration (0.1–0.5 mol/l). The solution became clear and homogeneous after stirring for about 20–30 min. The molar ratio DEA/Zn was fixed to 1.0 as employed by Takahashi et al. [19]. The sols prepared with a concentration up to 0.2 mol/l are very stable. For higher concentration a crystalline precipitation occurs after a few days.

Fig. 1 shows also a flow chart of the coating procedure.

* Corresponding author. Tel.: +49-681-9300-317; fax: +49-681-9300-249.

E-mail address: aegerter@inm-gmbh.de (M.A. Aegerter)

0040-6090/99/$ - see front matter
PII: S0040-6090(99)00211-4

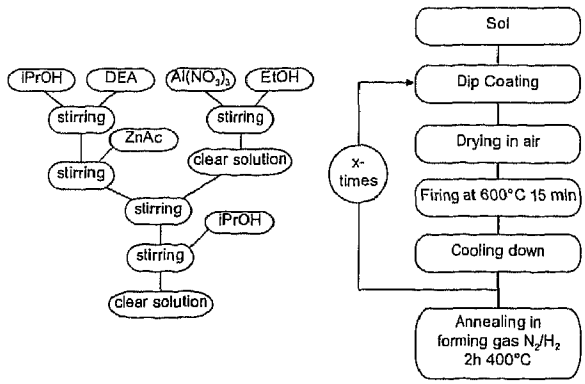

Fig. 1. Flow chart of the preparation of the coating solution (left) and coating procedure for ZnO:Al multilayer coatings.

ZnO:Al coatings have been prepared by dip-coating 1.1 mm thick alkali free glass (AF45 DESAG, slide dimensions 60 × 100 mm^2) at a withdrawal speed of 5 mm/s and heating the sample directly in a furnace at 600°C for 15 min. The coating process was repeated after cooling down to room temperature in order to increase the thickness of the coatings.

All samples have been tempered in a furnace under forming gas flux (95 N_2/5H_2) of 200 l/h to decrease the resistivity. The samples were heated from room temperature to 400°C at a rate of 500°C/h, held at this temperature for 2 h and cooled down to 37°C by convection under forming gas flux.

3. Experimental

Thickness measurements were performed with a Stylus Profiler (Tencor P10). The electrical properties have been measured with the van der Pauw and Hall method (MMR Technologies) with an applied magnetic field of 1.3 T. For X-ray diffraction (XRD) measurements a Siemens D500 equipment with a thin film attachment was used. 2θ-scans from 20 to 65° were performed at grazing incidence

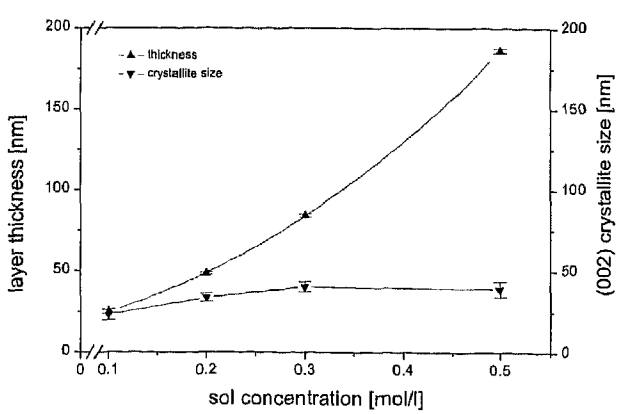

Fig. 2. Thickness and crystallite size of single layer ZnO:Al versus concentration of the sol. The lines are drawn as a guide for the eyes.

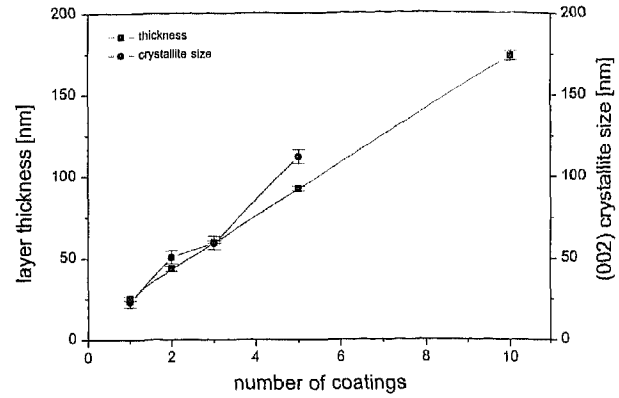

Fig. 3. Thickness and crystallite size of multilayer ZnO:Al coatings obtained with the 0.1 M sol versus the number of coatings. The lines are drawn as a guide for the eyes.

(θ = 2°). The crystallite size was calculated from the FWHM of the (002) peak corrected for the instrumental line width broadening using the Scherrer equation [21]. Optical measurements were performed with a Varian Cary5E double beam spectrometer. An absolute specular reflectance accessory (VW-Geometry) was used for near normal (7°) reflection measurements in the range from 200 to 3000 nm. Transmission electron microscopy (TEM) was done with a Philips CM200FEG using cross-sectional preparation.

4. Results

4.1. Structural Properties

The variation of single layer thickness with the concentration of the coating solution is plotted in Fig. 2. A non-linear dependence of the film thickness on the concentration is observed. Fig. 3 shows the thickness of the films as a function of the number of coatings obtained with the 0.1 M solution. After the first layer deposition the thickness of the coating increases linearly (16.4 nm/layer) with the number of layers.

All samples are polycrystalline and exhibit the zincite structure (JCPDS 36–1451) with all peaks in the recorded range identified. The crystallite size of single layer coatings is saturated at 40 nm (Fig. 2), whereas that of multilayer coatings increases linearly with the number of coatings up to five layers (Fig. 3). Coatings with more than five layers exhibit larger crystallite size (Section 4.2.) but their determination using the Scherrer procedure is not reliable as the line width is then essentially governed by the instrumental line width.

Various authors have reported a preferential orientation of the crystallites even for sol gel AZO layers [12–15,17,19]. The texture coefficient, TC, was calculated for all our samples from the diffraction spectra following Kim [22]:

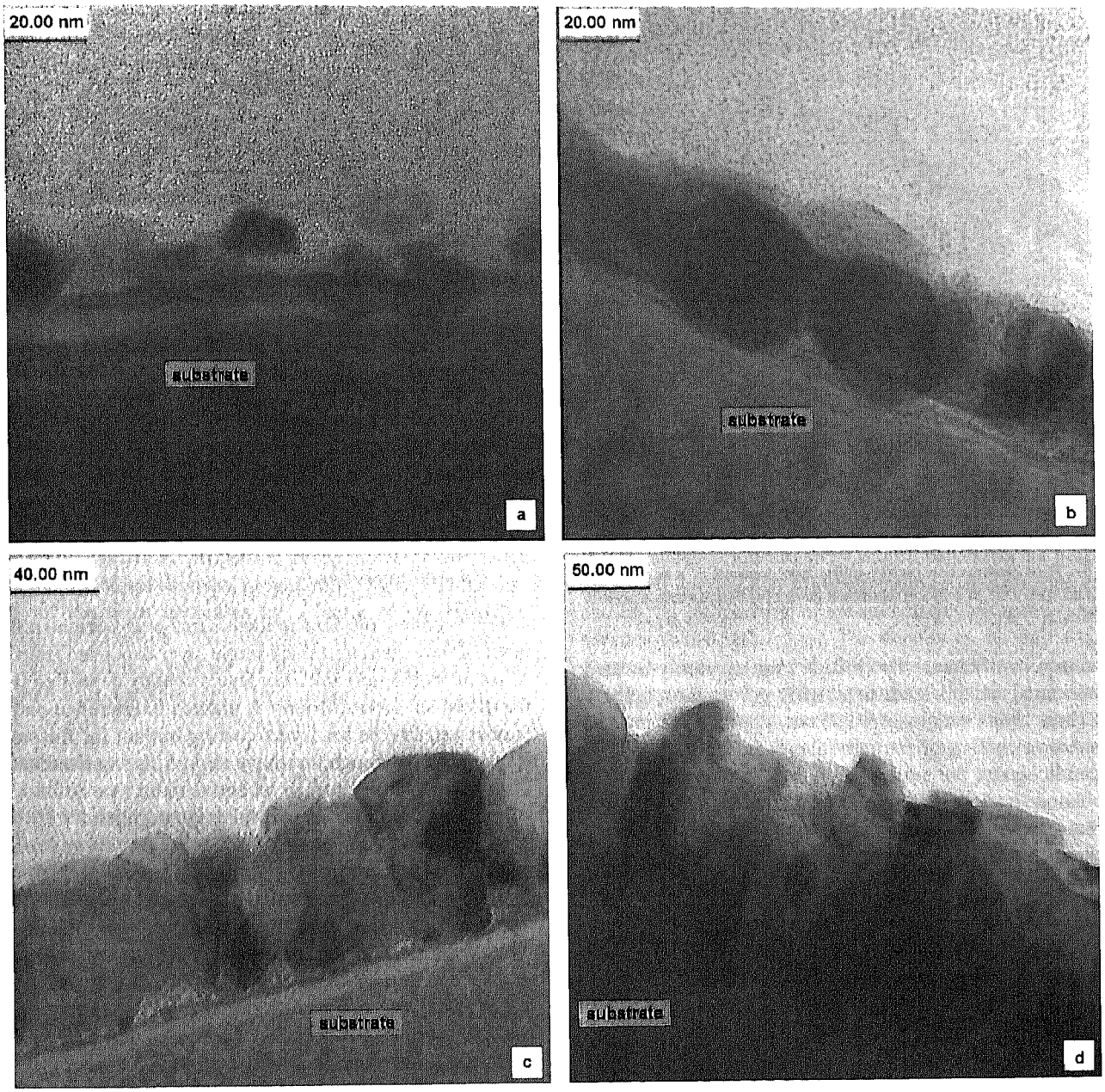

Fig. 4. TEM cross section pictures (diffraction contrast) of (a) one layer (b) two layers (c) five layers (d) ten layers of ZnO:Al coatings obtained with the 0.1 M (0.6 at.%) solution. An evolution from spherical to columnar growth is observed with increasing number of layers.

$$\mathrm{TC}(hkl) = \frac{I(hkl)/I_0(hkl)}{1/N \cdot \sum nolimits_N [I(hkl)/I_0(hkl)]} \quad (1)$$

where $I(hkl)$ and $I_0(hkl)$ denotes the measured intensity and the intensity of the standard powder diffraction pattern (JCPDS 36-1451), respectively. A slight texture with the (002) orientation perpendicular to the substrate was observed for single layers (TC = 2.8–1.9) and for multilayers (TC = 2.8–1.8).

4.2. Morphology

The morphology of one, two, five and ten layer coatings obtained with the 0.1 M sol is shown by TEM cross-sectional preparation (Fig. 4a–d). The single layer coating consists of spherical particles with 15–25 nm in diameter scattered over the surface of the substrate. The two layer coating also consists of spherical particles but with a larger diameter (25–35 nm). The size of the particles is comparable to the thickness of the coating (Fig. 4a,b). A columnar growth perpendicular to the surface is observed for the five and ten layer coatings (Fig. 4c,d).

Thick single layers prepared from the 0.5 M sol (Fig. 2) do not show a columnar growth but consist of spherical crystalline particles of about 40 nm in diameter (Fig. 5). The size of the particles is smaller than the thickness of

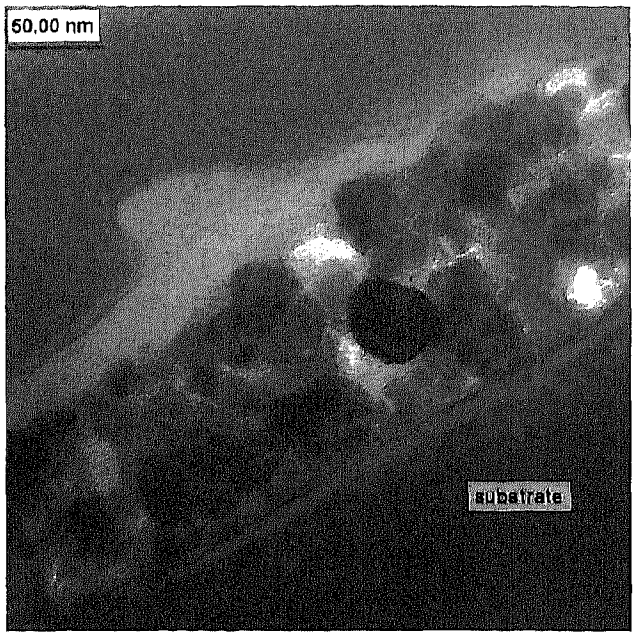

Fig. 5. TEM cross section picture (diffraction contrast) of a single layer obtained with a 0.5 M solution (thickness determined from surface profiler is 186 nm).

the film ($d = 186$ nm). The particles are randomly located and oriented and this leads to a highly porous morphology.

A three layers sample ($d = 125$ nm) deposited from a 0.2 M solution consists of particles elongated in the direction perpendicular to the surface (Fig. 6). The crystallite size calculated from the (002) peak is 65 nm.

From these data one estimates a 'critical single layer thickness' of ca. 15–20 nm necessary to observe a columnar

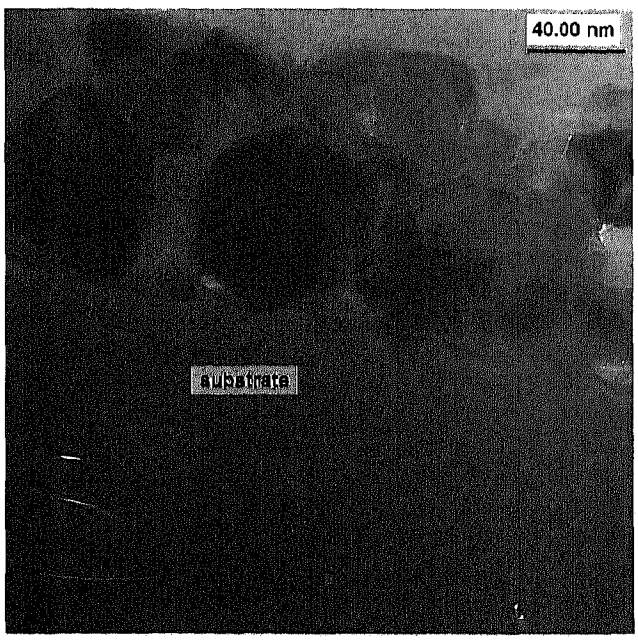

Fig. 6. TEM cross section picture (diffraction contrast) of three layers of ZnO:Al obtained with a 0.2 M solution ($d = 125$ nm).

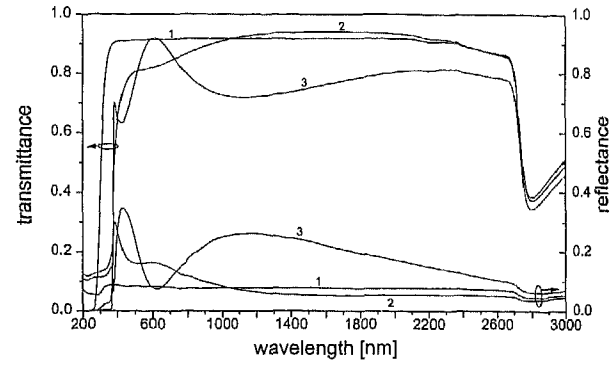

Fig. 7. Transmittance and near normal (7°) reflectance of substrate (1), AZO single layer ($d = 186$ nm) obtained from 0.5 M solution (2) and ten layers AZO coating ($d = 174$ nm) obtained from 0.1 M solution (3).

growth of ZnO:Al coatings for this particular dopant concentration (0.6 at.%). This value is roughly half the crystallite size of thick single layers (Fig. 2).

4.3. Optical properties

Fig. 7 shows the transmittance and near normal reflectance of the substrate, a thick single layer deposited from 0.5 M sol ($d = 186$ nm) and a ten layers coating deposited from the 0.1 M sol ($d = 174$ nm). A marked interference pattern is observed for the ten layers coating but not for the single layer coating although they have almost the same thickness. This is due to differences in refractive index (see below) and possibly due to differences in surface roughness.

Photopic and direct solar transmittance (τ_v, τ_e) and reflectance (ρ_v, ρ_e) were calculated following [23]. The values are listed in Table 1. The high photopic transmittance of the ten layers sample is due to the marked interference occurring at the maximum of the human eye sensitivity.

The refractive index at 550 nm of single and multilayer coatings is given in Fig. 8. It was determined by fitting the transmittance and reflectance spectra of the appropriate sample with a model consisting of a Drude contribution in the infrared and a Campi model [24] for the bandgap region using the SCOUT98 computer program [25]. All single layer spectra except the one obtained with the 0.5 M sol and all multilayer spectra were fitted with a standard deviation ranging from 2 to 6×10^{-4}. The single layer refractive index is small ($n = 1.74$) and decreases with the sol concentration (Fig. 8 lower curve) indicating a decrease of the film density. On the other hand the refractive index of the multilayer coatings increases from 1.74 to 1.95 as the number of coatings increases, the maximum value being still smaller than that of zinc oxide single crystal ($n = 2.02$ [26]). This indicates an increase of the film density, which can also be observed from TEM pictures (Fig. 4a–d).

4.4. Electrical properties

The electrical properties of single layer coatings obtained

Table 1
Photopic and direct solar transmittance and reflectance for AZO single and multilayer coatings. The error from experimental uncertainty of ± 0.1% at the single wavelength was estimated to ± 2.0% and ± 3.0% for photopic and solar value, respectively

Sol Concentration (mol/l)	Number of layers	Photopic transmittance τ_v (%)	Solar transmittance τ_e (%)	photopic reflectance ρ_v (%)	solar reflectance ρ_e (%)
0.1	1	89.0	10.9	88.9	9.7
0.1	2	81.2	18.4	83.8	14.2
0.1	3	73.6	26.0	79.1	18.5
0.1	5	68.2	30.5	74.1	22.5
0.1	10	86.4	14.1	75.3	20.4
0.2	1	84.1	13.7	85.5	11.4
0.3	1	80.7	17.1	84.0	12.6
0.5	1	81.3	16.2	84.2	11.8

with different sol concentration are presented in Fig. 9. The resistivity shows a minimum for coatings made with the 0.2 M solution. The carrier density decreases with the increase of the sol concentration, whereas the mobility shows a maximum at 0.2 M and a constant value for higher concentrations. The electrical properties of multilayers deposited from the 0.1 M solution are presented in Fig. 10. The resistivity of the films decreases by a factor of 10^2 with the number of coatings. This variation is almost essentially due to the strong increase of the mobility as the carrier concentration increases only by a factor of 1.5.

5. Discussion

Different morphologies have been observed in ZO and AZO coatings made by the sol gel process. A columnar growth was reported for undoped zinc oxide multilayer coatings with an individual layer thickness of ca. 20 nm [14,18]. However, for AZO coatings only a layered structure with spherical grains [17] or a homogeneous distribution of spherical grains [15] have been observed. Usually the coatings present no texture or are slightly textured [16,17,19] but Ohyama et al. [13–15] have reported a complete preferential orientation of the crystallites with the (002) direction perpendicular to the surface when monoethanolamine (MEA) was used as sol stabiliser.

The morphology and texture of AZO coatings made by the sol gel process appears therefore to be dependent on the coating procedure and still unidentified parameters. The results presented in this paper have shown that the morphologies can be tailored from an agglomeration of spherical particles to a columnar type of arrangement and that these structures have an important influence on the electrical properties of the coatings.

Single layers are always made of an agglomeration of spherical particles with a high void fraction and consequently a low density (Figs. 4 and 5). For very thin single layer (<ca. 20 nm) heterogeneously nucleated crystals predominate [30] and their size is limited by the thickness of the layer (Fig. 2). As the single layer thickness increases the formation of homogeneously nucleated crystals becomes more likely. Consequently the size of the particles and crystallites increase only slightly and reaches a saturation value of about 40 nm (Fig. 2) for our sintering conditions which are thought to be in a low temperature range, where the nucleation rate is higher than the growth rate [30]. However this saturation value should depend on the process parameter (drying and firing temperature, heating rate, etc.) and on the composition of the sol (dissolving agent, type of precursors and stabilisers). The density of the single layer coatings decreases as their thickness increases as indicated by the results of the refractive index (Fig. 8). As a consequence the carrier concentration slightly decreases by a factor of 2 (Fig. 9). The carrier mobility (Fig. 9) shows a peculiar behaviour. It is governed by the particle size, the number of the grain boundaries and the surface roughness. The effective carrier concentration μ_{eff} can be written as [31].

$$\frac{1}{\mu_{eff}} = \sum_i \frac{1}{\mu_i} \tag{2}$$

where μ_i are the contributions to the mobility from different scattering mechanisms. In very thin single layer (<ca. 20 nm) the heterogeneously nucleated spherical particles are small and scattered over the substrate surface and exhibit almost no contact between them (Fig. 4a) leading to a very low mobility ($\mu < 1$ cm^2/Vs Fig. 9). As the thickness increases to ca. 50 nm, however, the mobility increases and passes through a maximum ($\mu = 6$ cm^2/Vs). In this range (20–50 nm) the particles are predominantly heterogeneously nucleated and arrange themselves into a 2-D network which eventually becomes densely packed with increase of the film thickness, minimising the grain boundary scattering and consequently increasing the mobility. As the single layer thickness becomes larger than 50 nm the homogeneously nucleated particles predominate. The crystallite growth is limited to ca. 40 nm in diameter by the high nucleation rate and a 3D network of randomly distributed particles is formed. This morphology increases the grain boundary scattering leading again to a slightly decreased mobility ($\mu = 4$ cm^2/Vs). This explains the minimum in

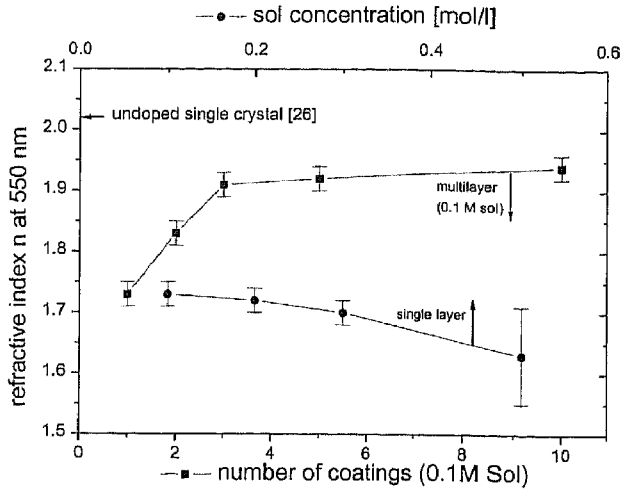

Fig. 8. Refractive index of AZO single and multilayer coating calculated from transmittance and near normal (7°) reflectance spectra (200–3000 nm) with the Campi and Drude model.

resistivity observed for single layer coatings made with the 0.2 M sol.

A completely different morphology has been obtained in multilayer coatings made of very thin individual layers. If the thickness of the individual layers is kept small enough the formation of heterogeneously nucleated crystals is enhanced at the interface of the last sintered layer and the gel film and a columnar growth takes place. This occurs only if the individual layer thickness is smaller or equal to ca. 20 nm. The randomly orientated faces of the crystallites of the first layer serve as nuclei for the columns (Fig. 11). This columnar growth increases the crystallite size perpendicular to the surface and consequently increases the density of the film as indicated by the increase of the refractive index with the number of coatings (Fig. 8). Following the above argumentation the carrier density increases only slightly with the number of coatings by a factor of 1.5. The strong increase in mobility up to a value of 42 cm^2/Vs as the number of deposited layers increases (Fig. 10) is attributed to the higher mean free path and the lower surface

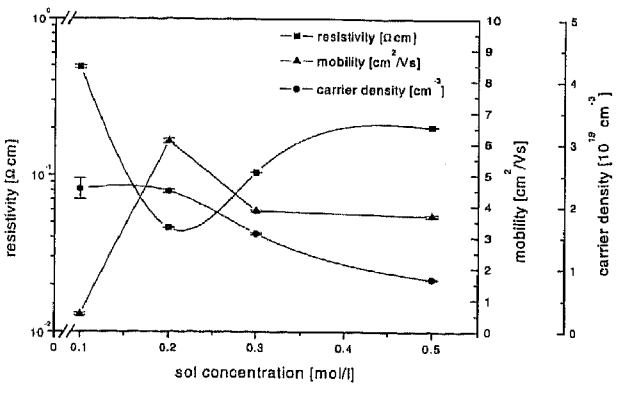

Fig. 9. Electrical properties of single layer ZnO:Al coatings as a function of the concentration of the sol. The lines are drawn as guides for the eyes.

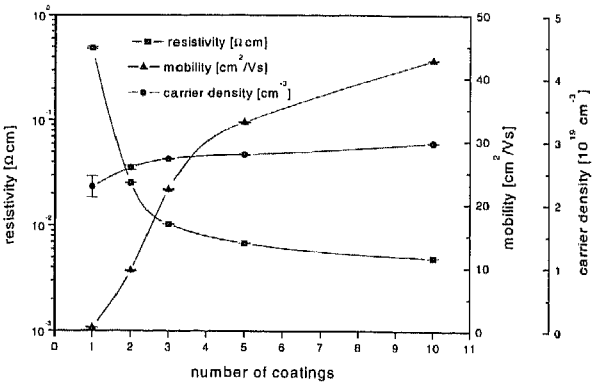

Fig. 10. Electrical properties of multilayer ZnO:Al coatings obtained with the 0.1 M sol as a function of the number of coatings (each layer is ca. 17 nm thick). The lines are drawn as guides for the eyes.

scattering of the electrons. From the relation

$$\rho_{ee} = \frac{1}{ne\mu} \tag{3}$$

it is evident that the electrical resistivity is decreased mainly by the increase in mobility for the columnar grown sol gel coatings.

The large difference between the indices of refraction observed for the two morphologies also explains the presence or absence of an interference pattern in the optical transmission spectra of a multilayer ($n = 1.94$) and a single layer coating ($n = 1.65$) of almost the same thickness ($d \cong 180$ nm, Fig. 7). Another contribution, which was not investigated, could have been the surface roughness.

A layered structure with a highly densified thin region at the top interface of each individual layer was observed for antimony doped tin oxide (ATO) [27]. However a recent study revealed that a columnar growth is also observed for multilayer coatings made with very thin layers [28]. A similar result was obtained by Takahashi et al. [29] for dip coated tin doped indium oxide thin films. For columnar grown TiO_2 multilayer coatings a similar model including a critical nucleus size was proposed by Ohya [18].

Our single and multilayer AZO coatings present only a small texture with the c-axis perpendicular to the surface of the substrate in contradiction with the results of Ohyama et al. [13–15] who were able to obtain fully oriented multilayer coatings. The reason of these difference in texture is not yet clear. The use of monoethanolamine as a sol stabiliser as well as the aluminium doping [18] may have reduced the size of the particles to a too small value for that coating process impeding a columnar growth but favouring a full orientation of the crystallites. Nevertheless the best resistivity obtained by using those two different sols and coating processes is almost the same: 6.5×10^{-3} Ω cm for a homogeneous distribution of spherical particles with highly preferential orientation [15] and 5×10^{-3} Ω cm for a columnar morphology of slightly oriented particles. Both, columnar morphology or preferential orientation of the crystallites

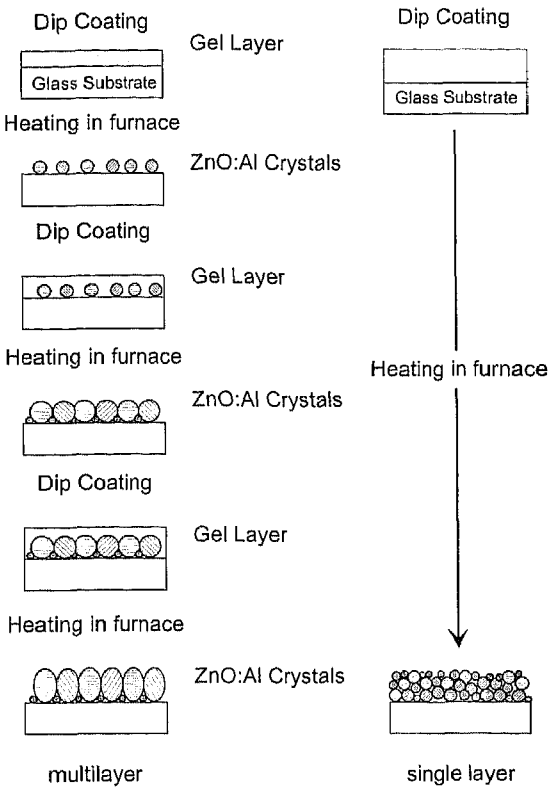

Fig. 11. Scheme of the crystal growth observed in single and multilayer sol gel AZO coatings. Thick gel films lead to spherical crystallites randomly oriented whereas thin gel films lead to a columnar growth.

lead to low resistivity AZO sol gel coatings. However a fully oriented columnar morphology should present even a lower resistivity.

6. Conclusion

AZO sol gel multilayer coatings have been prepared with electrical resistivity as low as 5×10^{-3} Ω cm and good optical properties. The electrical properties of the coatings have been related to the structural and morphological properties of the coatings. As long as homogeneous nucleation takes place predominantly the particles are spherically shaped and randomly distributed. Therefore the film density is low and the resistivity is high. Heterogeneous nucleation is favoured by depositing very thin individual layers leading to a columnar growth of the particles. In this case the film density is high and the resistivity is low. Columnar growth promotes a low resistivity of the coating. Highly preferential orientation of the particles was not achieved but is expected to decrease the electrical resistivity even more. Probably the particular morphology observed here for AZO coatings can be obtained with other sol gel materials.

Acknowledgements

The authors are grateful to Dr. T. Krajewski for the TEM pictures. This work was financed in part by BMBF (Förderzeichen 2A67/03 N 9040) and the State of Saarland (Germany).

References

[1] J.A. Anna Selvan, H. Keppner, A. Shah, Mater. Res. Soc. Symp. Proc. 426 (1996) 497.
[2] M. Ritala, T. Asikanen, M. Leskelä, J. Skarp, Mater. Res. Soc. Symp. Proc. 426 (1996) 513.
[3] V. Gupta, A. Mansingh, J. Appl. Phys. 80 (2) (1996) 1063.
[4] M. Bertolotti, M.V. Laschena, M. Rossi, A. Ferrari, L.S. Qian, F. Quaranta, A. Valentini, J. Mater. Res. 5 (9) (1990) 1929.
[5] K.-S. Weißenrieder, J. Müller, Thin Solid Films 300 (1997) 30.
[6] J.L. Deschanvres, B. Bochu, J.C. Joubert, J. Phys. 4 (3) (1993) 485.
[7] S. Hayamizu, H. Tabata, H. Tanaka, T. Kawai, J. Appl. Phys. 80 (2) (1996) 787.
[8] B. Szyszka, S. Jäger, J. Non-Cryst. Solids 218 (1997) 74.
[9] T. Nakada, N. Murakami, A. Kunioka, Mater. Res. Soc. Symp. Proc. 426 (1996) 411.
[10] J. Aranovich, A. Ortíz, R.H. Bube, J. Vac. Sci. Technol. 16 (4) (1979) 994.
[11] P. O'Brien, T. Saeed, J. Knowles, J. Mater. Chem. 6 (7) (1996) 1135.
[12] K. Nishio, S. Miyake, T. Sei, Y. Watanabe, T. Tsuchiya, J. Mater. Sci. 31 (1996) 3651.
[13] M. Ohyama, H. Kozuka, T. Yoko, S. Sakka, J. Ceram. Soc. Jpn. 104 (1996) 296.
[14] M. Ohyama, H. Kozuka, T. Yoko, Thin Solid Films 306 (1997) 78.
[15] M. Ohyama, H. Kozuka, T. Yoko, J. Am. Ceram. Soc. 81 (6) (1998) 1622.
[16] W. Tang, D.C. Cameron, Thin Solid Films 238 (1994) 83.
[17] Y. Ohya, H. Saiki, Y. Takahashi, J. Mater. Sci. 29 (15) (1994) 4099.
[18] Y. Ohya, H. Saiki, T. Tanaka, Y. Takahashi, J. Am. Ceram. Soc. 79 (4) (1996) 825.
[19] Y. Takahashi, M. Kanamori, A. Kondoh, H. Minoura, Y. Ohya, Jpn. J. Appl. Phys. 33 (1994) 6611.
[20] H. Nanto, T. Minami, S. Shooji, S. Takata, J. Appl. Phys. 55 (4) (1984) 1029.
[21] M.N Rahaman, Ceramic processing and sintering. Materials engineering, Vol. 10, Marcel Dekker, New York, 1995.
[22] K.H. Kim, J.S. Chun, Thin Solid Films 141 (1986) 287.
[23] DIN-EN-410, Glass in Building; Determination of light transmittance, solar direct transmittance, total solar energy transmittance, ultraviolet transmittance and related glazing characteristics; German Version prEN410: 1990 – ENTWURF, 1991, Deutsches Institut für Normung e. V, Berlin.
[24] D. Campi, C. Coriasso, J. Appl. Phys. 64 (8) (1988) 4128.
[25] W. Theiß, SCOUT 98, Soft Science, Aachen, Germany, 1998.
[26] V. Srikant, D.R. Clarke, J. Appl. Phys. 83 (10) (1998) 5447.
[27] M.A. Aegerter, A. Reich, D. Ganz, G. Gasparro, J. Pütz, J. Non-Cryst. Solids 218 (1997) 123.
[28] G. Gasparro, private communication.
[29] Y. Takahashi, S. Okada, R. Bel Hadj, Y. Tahar, K. Nakano, T. Ban, Y. Ohya, J. Non-Cryst. Solids 218 (1997) 129–134.
[30] G.W. Scherer, J. Sol-Gel Sci. Technol. 8 (1997) 353.
[31] H. Haijtema, Ph.D. Thesis, University of Delft, Netherlands, 1989, p. 44.